A study of hydrogen desorption from $Fe_{55}Cr_{25}Ni_{20}$ alloy by means of ferromagnetic resonance

1996 J. Phys.: Condens. Matter 8 1831

(http://iopscience.iop.org/0953-8984/8/11/025)

J. Phys.: Condens. Matter **8** (1996) 1831–1844. Printed in the UK

A study of hydrogen desorption from $Fe_{55}Cr_{25}Ni_{20}$ alloy by means of ferromagnetic resonance

B D Shanina†, S P Kolesnik†, A A Konchitz†, V G Gavriljuk‡ and A V Tarasenko‡

† Institute of Semiconductor Physics, 252028 Kiev, Ukraine
‡ Institute of Metal Physics, 252142 Kiev, Ukraine

Received 20 April 1995, in final form 22 November 1995

Abstract. FMR absorption in hydrogen-charged $Fe_{55}Cr_{25}Ni_{20}$ austenitic alloys was measured versus temperature in the range of 4–200 K and at 77 K versus duration of hydrogen desorption caused by heatings at 293–393 K. Under the influence of hydrogen the FMR signal is shifted towards high magnetic fields, which provides evidence for the increasing role of s electrons in the formation of the magnetic structure of the alloy, and broadened, the latter effect being caused by the effective electron scattering of the hydrogen atoms. The FMR intensity is found to be proportional to the saturation magnetization and obeying the $T^{3/2}$-law at low temperatures ($T \ll \Theta_C$, where Θ_C is Curie temperature).

The activation enthalpy E_a and the frequency factor ω_0 were measured from the dependence of the integral intensity and the line width recorded at 77 K on the duration of desorption at various temperatures. The value of $E_a = 0.56 \pm 0.02$ eV is consistent with the data for hydrogen migration in the same alloy obtained by means of the internal-friction technique while the value of the frequency factor $\omega_0 = (3.0 \pm 0.1) \times 10^6$ s^{-1} reflects the peculiarities of the hydrogen-induced magnetic structure of the alloy. It characterizes the length of the spin correlation of s electrons which determines the distance of hydrogen atom migration needed for a detectable change of the magnetic structure during hydrogen desorption. The results indicate the strong s–d exchange interaction between hydrogen s electrons and the host atoms.

1. Introduction

Hydrogen significantly changes the physical and mechanical properties of transition metals and their alloys (see, e.g., [1–3]). As a rule, hydrogen atoms are easily dissolved in metals, being at the same time extremely mobile in solid solution, which causes the serious problem of hydrogen embrittlement in engineering materials.

Iron-based FCC alloys (stainless austenitic steels) are usually regarded as hydrogen-resistant engineering materials. The activation enthalpy of hydrogen migration in FeCrNi alloys is relatively high (0.52–0.57 eV [4] in comparison with, e.g., 0.4 eV for H in Ni [5]), this being the reason for low hydrogen permeability and, as a result, a long life under hydrogen attack. Nevertheless, the brittle fracture of CrNi austenitic steels occurs under high hydrogen gaseous pressure or cathodic charging, and numerous studies of the mechanisms of their hydrogen embrittlement are under way (see [1–3] and also [6–8]). The hydrogen content (hydrogen/metal atomic ratio) in iron-based FeCrNi austenites introduced by cathodic charging or high-pressure hydrogenation has been found to be within the range 0.4–0.7 [9–11]. Therefore, the effects of hydrogen on physical properties are expected to

0953-8984/96/111831+14$19.50

be significant and the knowledge of the hydrogen state in FeCrNi alloys is important from both physical and practical points of view.

This study is aimed at obtaining information on hydrogen behaviour in FeCrNi FCC alloy (austenite). So far the physical aspects of hydrogenated austenites have been mainly studied using an internal-friction technique which allows one to observe an elastic relaxation of hydrogen-induced noncubic defects in FCC crystal lattice (see, e.g., [12–15]). The occurrence of the orientation dependence of the relaxation strength measured on single crystals and the values of the activation parameters obtained from the frequency shift have led to the conclusion that relaxation is caused by reorientation of 'substitutional-solute–hydrogen-atom' complexes due to diffusion jumps of the hydrogen atoms. The activation enthalpy of relaxation was consistent with that of hydrogen migration in austenite while the frequency factor corresponded to one or several jumps of the hydrogen atom for the relaxation time, giving evidence for different kinds of substitutional–interstitial complex in hydrogenated austenite [15].

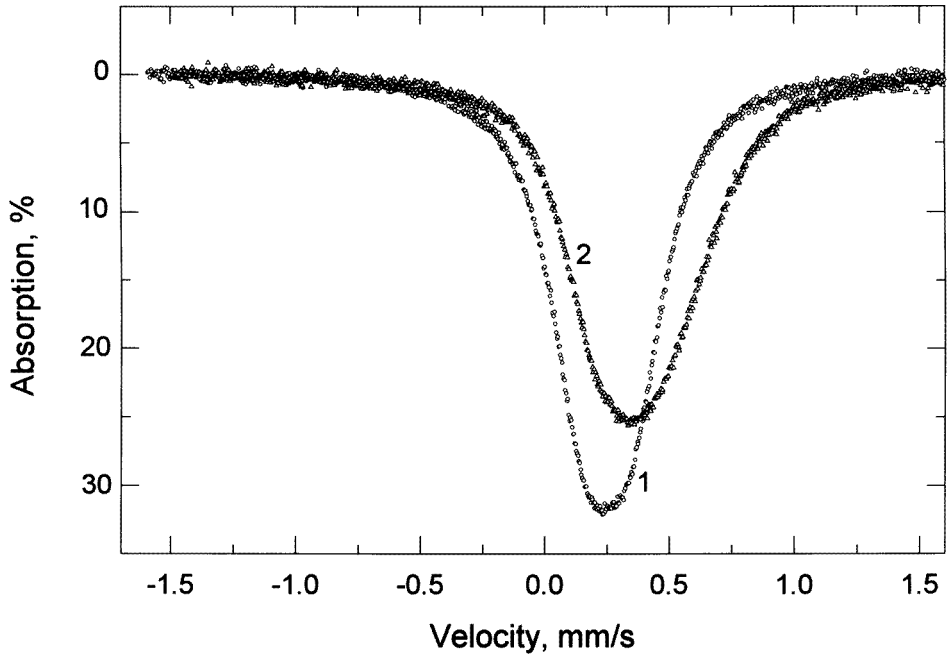

Figure 1. Mössbauer spectra of $Fe_{55}Cr_{25}Ni_{20}$ alloy before (1) and after (2) hydrogen charging. $T = 88$ K.

In the present study we used the effect of hydrogen on the electronic and magnetic structure of iron-based austenites and made an attempt to obtain information on hydrogen-induced magnetism and hydrogen migration during its desorption using ferromagnetic resonance. The following factors seem to suggest that the study will be successful.

The resonance absorption of the microwave power in ferromagnetic material (ferromagnetic resonance) is controlled by several material constants: the saturation magnetization M, the conductivity of the metallic sample σ, the Landau–Lifshitz constant of damping λ, and the exchange interaction constant A [16–18]. Hydrogen dissolved in the FCC lattice of the iron-based alloy must affect all of the above parameters. It is also known

[19] that, in Fe–Cr–Ni alloy, the value of the *g*-factor is different for d and s electrons, and, according to [20], the FMR resonance frequency depends on the magnetizing of s electrons by d electrons. The change of the s- and d-electron density ratio caused by hydrogen must affect the intensity of the FMR signal, too.

Table 1. Values of the resonance fields (the error of the measurements is ±0.004 T) and FMR line widths (the error of the measurements is ±0.001 T) for parallel and orthogonal orientations of the magnetic field with respect to the sample plane after hydrogen charging ($t = 0$) and after prolonged hydrogen desorption (t_1—its values are shown in the final column). The measurements were performed at 77 K.

		$t = 0$		$t = t_1$		
Number of the sample	T_{heat} (K)	$H_\parallel$ $\Delta H_{p-p,\parallel}$ (T)	$H_\perp$ $\Delta H_{p-p,\perp}$ (T)	$H_\parallel$ $\Delta H_{p-p,\parallel}$ (T)	$H_\perp$ $\Delta H_{p-p,\perp}$ (T)	t_1 (min)
N1	273	0.272 0.101	0.358 0.124	0.297 0.062	0.327 0.073	140
N2	283	0.210 0.156	0.490 0.249	0.304 0.062	0.334 0.070	140
N3	300	0.280 0.109	0.389 0.148		0.330 0.062	40
N4	323	0.280 0.093	0.366 0.124	0.296 0.062	0.331 0.062	4
N5	348	0.272 0.109	0.366 0.124	0.303 0.047	0.334 0.062	1
N6	373	0.296 0.065	0.331 0.078	0.296 0.054	0.331 0.055	0.67
Before hydrogen charging	$T_{measure}$ 77(K)	0.132 0.175	0.202 0.175	— —	— —	—

Fe–Cr–Ni alloys containing 15–25% of chromium and 10–40% of nickel are weak ferromagnetics because of their FCC lattice structure and opposite directions of the atomic magnetic moments of Cr and Ni atoms (see, e.g., [16]). The Mössbauer spectra of the $Fe_{55}Cr_{25}Ni_{20}$ alloy chosen for investigation are presented in figure 1 as evidence for the weak ferromagnetism. Hydrogen charging causes a positive isomeric shift and some magnetic broadening of the singlet which is fitted with Zeeman's sextuplet having the hyperfine field $H_e = 1.14$ T (0.74 T before charging; compare, e.g., with $H_e = 33.3$ T for the strong ferromagnetic, BCC Fe). The small difference between the FMR resonance magnetic fields in parallel and orthogonal orientations of $\boldsymbol{H}_0$ with respect to the sample plane (see table 1) also confirms the weak ferromagnetism of the samples studied here.

For the weak ferromagnetics the integral intensity of the FMR signal $I(T)$ is proportional to the magnetization of the sample $M(T)$ at a given temperature T. The value of $M(T) = M_0 F(T/\Theta)$ [16], where $M_0 = N\mu_B$ is the saturation magnetization, N is the density of the magnetic moments, $F(T/\Theta)$ is a temperature function of the magnetization, and Θ is the Curie temperature. Therefore, if hydrogen affects the value of $M(T)$, this effect has to produce a change in the values of N and Θ. It is natural to expect that $I(T)$ varies with the change of the hydrogen concentration x as a power expansion in x: $I = I_0 + a_1 x + a_2 x^2 + \ldots$. While hydrogen is outgassing from the sample, the slowest of the exponents will represent the rate of hydrogen desorption at a given temperature. This

reveals an opportunity to study the activation energy of desorption and its dependence on different factors: chemical composition, magnetic structure, concentration of vacancies and dislocations, etc. The measurements of the temperature dependence of FMR parameters in the presence and absence of hydrogen in the samples make it possible to study the effect of hydrogen on the electronic and magnetic structures of the alloy.

As FMR is caused by excitation of the spin waves it is noteworthy that the kinetics of hydrogen desorption measured using FMR illustrates mobility of the hydrogen atoms which are localized in states related in some way to the electron density on the Fermi surface. This circumstance distinguishes the measurements in this study from those performed by means of internal friction [12–15]. The comparison of activation enthalpies and pre-exponential factors obtained by means of different experimental techniques will help to adjust the correlation between the measured thermodynamical parameters and different hydrogen states in solid solution.

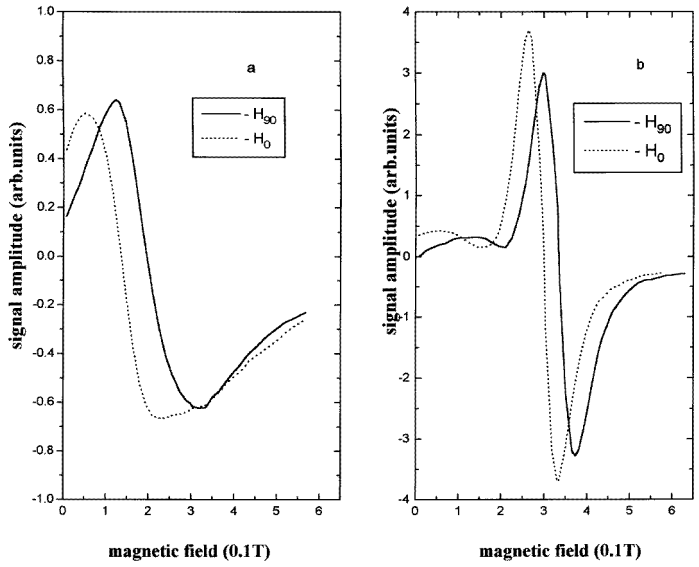

Figure 2. Signals of ferromagnetic resonance recorded at $\nu = 9.3$ GHz for the alloy $Fe_{55}Cr_{20}Ni_{25}$ before (a) and after (b) hydrogen charging.

2. Experimental procedure

A set of samples of $Fe_{55}Cr_{25}Ni_{20}$ alloy $4 \times 20 \times 0.068$ mm^3 in size were prepared by melting in vacuum, hot forging and cold rolling with intermediate annealings. The final homogenizing treatment was carried out in vacuum at 1150 °C for 30 min followed by quenching in water. Hydrogen charging was performed in 1N H_2SO_4 + 250 mg l^{-1} $NaAsO_2$ solution at the current density of 500 A m^{-2} for 72 hours. The hydrogen content in the samples was equal to 345 wt ppm (1.5 at. %). The samples were stored in liquid nitrogen before the FMR measurements were made; these were carried out using an electron paramagnetic resonance spectrometer at the frequency of 9.3 GHz.

For the purpose of measurements we selected samples with the same integral intensity of the hydrogen-induced FMR signal (see figure 2(*b*)), which corresponded to equal amounts

of hydrogen in the samples. In fact, the intensities of the FMR signal in samples having the same size and charged in the same conditions did not differ by more than 10%.

We have performed two kinds of measurement: (a) measurements of the temperature dependence of FMR line parameters made during the cooling of a sample from 200 K (below this temperature hydrogen atoms are immobile in this alloy for the duration of the measurements; see, e.g., [14, 15]) up to 4 K; and (b) temperature–time measurements at 77 K after heating and exposing the sample at various temperatures.

The permanent temperature measurements of the FMR signal integral intensity were performed immediately after cathodic charging and also after exposure of the hydrogen-charged sample at 292 K for 50 min. The intensity of the signal was fourfold decreased after exposure at 292 K; however, we could still observe a sufficiently intensive FMR line caused by hydrogen. In both cases—that of the freshly charged sample and that of one that had been subjected to partial outgassing at 292 K—the FMR signal parameters were measured in the temperature range of 4–200 K. The temperature dependence of the sample magnetization provides information about the character of the magnetic structure in the sample. In making these measurements of the samples with different hydrogen contents we pursued two objectives. The first is concerned with the need to prove that the integral intensity of the signal is proportional to the saturation magnetization of hydrogen-charged samples. The second was to test the difference between the magnetic properties of samples with high and low contents of hydrogen.

During the temperature–time measurements the FMR signal was recorded at 77 K, after which the sample was submerged in water at a fixed temperature, T_h, kept at this temperature for the time t_i and transferred again into liquid nitrogen to measure the FMR signal. Such heating at a fixed temperature was conducted many times ($i = 1, 2, 3, \ldots, N$ with N different for different temperatures) until hydrogen was desorbed out of the sample. This allowed us to measure the effect of the duration of the desorption process on the integral intensity of the FMR signal $I(t)$, the shift of the resonance magnetic field $(H_0 - H_{\mathrm{res}})$, where H_0 is the resonance field at the Larmor frequency of the conduction electron in the alloy, and the signal width, $\Delta H(t)$. The measurements were conducted on six identical samples at heating temperatures $T_h = 273$, 283, 300, 323, 348 and 373 K and the sample numbers in table 1 correspond to the annealing temperature number.

3. Results

In the absence of hydrogen all the samples show the broad band of absorption of the microwave-field power only (see figure 2(*a*)). The value of the resonance field which corresponds to the maximum of absorption is $H_{\mathrm{res},0} = 0.132$ T when the external magnetic field is directed along the sample plane and $H_{\mathrm{res},90} = 0.202$ T when the field is orthogonal to the sample plane. The line width which is equal to the distance between the extrema of the absorption derivative is $\Delta H_{p-p} = 0.175$ T. Prior to hydrogen charging the samples are weakly ferromagnetic and show a hysteresis of the microwave-field absorption characterized by the coercive force $H_C = 0.006$ T in the zero field.

Hydrogen charging causes the intensive resonance FMR line at the resonance frequency $\omega = g\beta H_{\mathrm{res}}$ with $H_{\mathrm{res},90}$ shifted towards the higher fields from the Larmor frequency of the free electron (figure 2(*b*)). This shows that, in the presence of hydrogen atoms, s electrons are magnetized more strongly by d electrons of the host atoms. Therefore, one can suppose a strong exchange interaction between s electrons of the hydrogen atoms and d electrons of the transition metal atoms.

A marked anisotropy of the resonance field is observed while anisotropy of the line

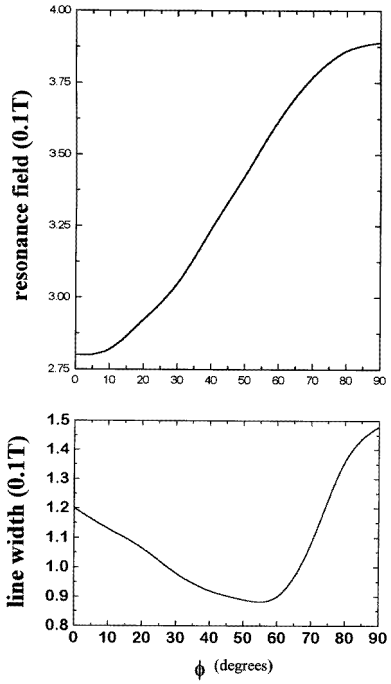

Figure 3. The dependence of the resonance-field value $H_{\rm res}$ and the line width ΔH_{p-p} of FMR on the orientation of the magnetic field with respect to the sample plane ($\phi = 90^\circ$ corresponds to the case of $\boldsymbol{H}$ perpendicular to the sample plane).

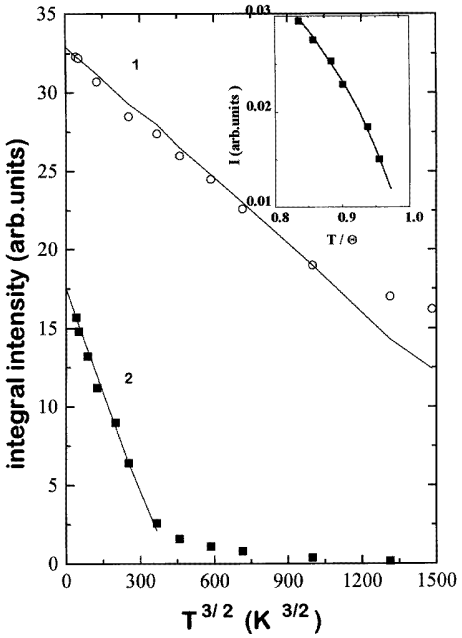

Figure 4. The temperature dependence of the integral intensity of the FMR signal as a function of $T^{3/2}$ for $T \ll \Theta_C$. The inset shows $I(t)$ in the vicinity of Θ_C as $(1 - T/\Theta_C)^{1/2}$, where $\Theta_C = 216$ K.

width is significantly smaller (see figure 3 and table 1). The weak anisotropy of the line width allows us to measure the values of the resonance fields using the zero position of the absorption derivative.

Typical values of the resonance fields for the parallel and orthogonal orientations of the magnetic field with respect to the sample plane are given in table 1 for each sample. The value of the resonance field of the FMR signal depends on the concentration of hydrogen which changes during its desorption. However, after lengthy desorption, when the FMR signal can still be reliably measured although the signal intensity has already decreased by one order of magnitude, further desorption does not affect the values of $H_{\rm res,0}$, $H_{\rm res,90}$ and the line width.

3.1. Permanent temperature measurements

The integral intensities of the FMR signals are presented for two samples in figure 4 as functions of $T^{3/2}$. Curve 1 was obtained for sample 3 with the initial hydrogen content induced by hydrogen charging, while curve 2 refers to the same sample after exposure at 292 K for 50 min. In the latter case the retained signal is still sufficiently intensive to register. As we have remarked above (see section 1), the integral intensity should have the same temperature dependence as the saturation magnetization in a weak ferromagnetic. It is known that the magnetization of iron-based ferromagnetic materials as $T \to 0$ is described

by the following function:

$$M = M(0)(1 - \alpha T^{3/2} - \beta T^{5/2}) \tag{1}$$

where $\alpha = \zeta(3/2)/(4\pi D)^{3/2}$, and $\beta = \zeta(5/2)/(4\pi D)^{5/2}$, and $\zeta(3/2)$ and $\zeta(5/2)$ are ζ-functions. Both of the experimental curves in figure 4 obey the $T^{3/2}$-law in the low-temperature range and do not reveal other possible slopes ($T^{5/2}$, T^2, T^3):

$$I_1 = 32.93(1 - 0.000\,42T^{3/2}) \qquad I_2 = 17.55(1 - 0.0025T^{3/2}). \tag{2}$$

Using (1) we found that $D_1 = 28.6$ K, $D_2 = 18.8$ K. Although the values of D in alloys are always significantly lower than the Curie temperature Θ_C, the ratio of D_1 to D_2 corresponds to that of Θ_C for the samples in cases 1 and 2, i.e. $\Theta_{C1}/\Theta_{C2} = 1.52$. For the sample with the high content of hydrogen (case 1) the range of high temperatures is far from the phase transition point, which prevents one from evaluating Θ_{C1}. However, for the sample with the small content of hydrogen (case 2) this evaluation was made on the assumption that in the vicinity of Θ_{C2} magnetization has to obey the law $(\Theta_C - T)^{1/2}$. We found that $\Theta_{C2} = 216$ K.

Thus, the integral intensity of the FMR signal is proportional to the magnetization of the sample. Figure 4 shows that both the Curie temperature and the saturation magnetization at 0 K are diminished with the decrease of hydrogen concentration. Therefore, in general, the change of integral intensity with time is not described by a one-exponential function.

Let us note that the $T^{3/2}$-law is consistent with the spin-wave nature of hydrogen-induced ferromagnetism. The temperature dependence of magnetization would have an exponential character if the hydrogen-induced magnetism could be described in terms of the Stoner bands as was supposed for hydrogenated Fe–Ni alloys in [21]. At the same time s electrons play a decisive role in the FMR measured here. This indicates a strong s–d interaction between the hydrogen s electrons and d electrons of the host atoms.

3.2. Temperature–time measurements

The results obtained from measurements of the integral intensity and the line width of FMR at $T = 77$ K versus duration t_h of the sample exposure at the temperature T_h of hydrogen desorption are shown in figure 5. The values of $I(t)$ and $\delta H_{p-p} = \Delta H_{p-p}(t) - \Delta H_{p-p}(t \to \infty)$ are given on logarithmic scales. It is clearly seen that the time law is an exponent with the same time constant for the intensity and the width of the FMR line. With the increase of T_h the time constant is markedly reduced, which is why in both panels of the figure the curves 1, 2, 3 are related to the upper x-axis (with the scale in minutes) while the curves 4, 5, 6 are related to the lower x-axis (with the scale in seconds), respectively.

Table 2. The exponential decay rate of the integral intensity (ω_I) and of the change of FMR line width ($\omega_{\delta H}$) with the heat treatment temperature of the sample.

T_{heat} (K)	273	283	300	323	348	373
ω (min^{-1})	0.0133	0.0288	0.0500	0.3400	1.1600	7.7300
$\omega_{\delta H}$ (min^{-1})	0.0074	0.0154	0.0468	0.4000	1.6000	5.5000

From the data shown in figure 5 the values of the exponential decay rate of the integral intensity and the line width were obtained (see table 2). The values of ω_I and $\omega_{\delta H}$ allow one to obtain the activation enthalpy of an elementary jump of the hydrogen atom on interstices in the crystal lattice and the pre-exponential frequency factor of the probability of such a

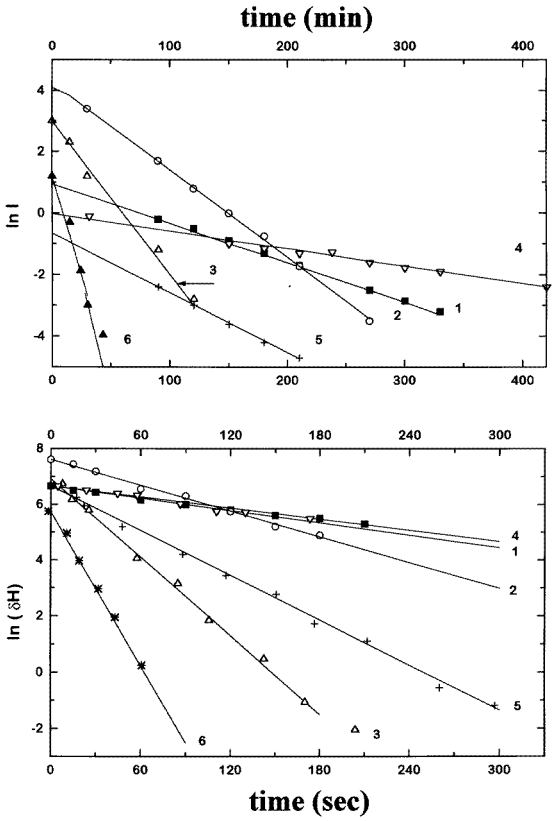

Figure 5. The dependence of the integral intensity of the FMR signal I and the line width $\delta H = (\Delta H(t) - \Delta H(t \to \infty))$ versus duration of the heating for sample i, where i is the number corresponding to T_{heat}; values of T_{heat} are given in table 1. The upper x-axes (in minutes) correspond to the curves 1, 2, 3; the lower axes (in seconds) correspond to the curves 4, 5, 6.

jump, by fitting the experimental data using the Arrhenius law. The Arrhenius plot for ω_I and $\omega_{\delta H}$ is shown in figure 6. The values of the enthalpy of activation E_a and the frequency factor ω_0

$$E_a = 0.56 \pm 0.02) \text{ eV} \qquad \omega_0 = (3.0 \pm 0.1) \times 10^6 \text{ s}^{-1} \tag{3}$$

were obtained from figure 6. The value 0.56 eV for the activation enthalpy is consistent with the data on hydrogen migration obtained for the same alloy by means of the internal-friction technique via hydrogen-induced Snoek-like relaxation [12–15] and is also within the limits of scattering of the hydrogen diffusivity data for CrNi austenitic steels evaluated from the permeability measurements [4]. However, the value of the frequency factor is significantly smaller than the value ω_{00} of about 10^{13} s^{-1} measured in the internal-friction studies, which unambiguously shows that by means of FMR we are dealing with hydrogen atoms bound to host atoms due to electron–electron interaction.

Our measurements of the FMR signal intensity performed over the wide temperature range did not reveal any signs of the presence of non-central interstitial hydrogen atoms in vibron states which could cause the temperature dependence of $I(T)$ at low temperatures to deviate from the $T^{3/2}$-law.

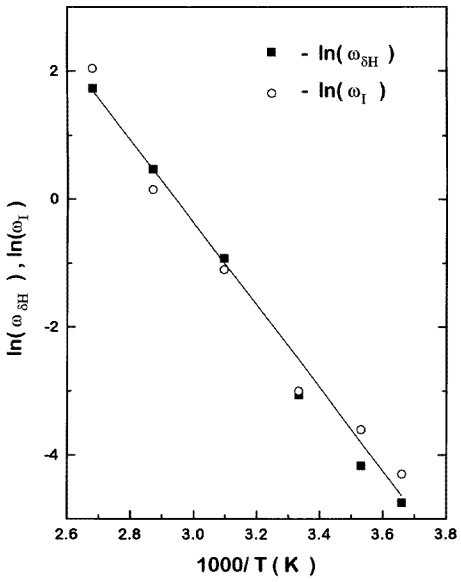

Figure 6. The temperature dependence of the hydrogen desorption rate for $Fe_{55}Cr_{20}Ni_{25}$ alloy measured on the basis of the changes of the integral intensity (circles) and of the FMR line width (solid squares).

4. Discussion

The line in figure 2(*b*) is due to presence of hydrogen only. It is absent before hydrogen charging and disappears during hydrogen desorption. This circumstance allows us to observe the change of magnetic structure in the course of hydrogen desorption. Let us discuss the hydrogen-induced magnetism in austenite on the basis of the change of FMR parameters caused by hydrogen.

4.1. Parameters of hydrogen-induced FMR

The theory of ferromagnetic resonance is based on the solution of Maxwell equations for the electromagnetic field, the Landau–Lifshitz equation for the magnetic moment of the sample, and the boundary conditions for the field and magnetization [16–18]. Below we will use the following dimensionless values: the field $\eta = H/4\pi H_i$, the Landau–Lifshitz damping constant $L = \lambda/4\pi H_i$, the extent of the exchange scattering in the electron system $\varepsilon = (A/2\pi H_i^2\delta^2)^{1/2}$, where δ is the depth of the skin layer, $\delta = c/(2\pi\omega\sigma)^{1/2}$, σ is the conductivity of the sample, ω is the the frequency of the microwave field, H_i is the inherent magnetic induction in the bulk of the sample, and $H_i = 4\pi M - H_A$, where $H_A = 2K_1/4\pi M$ is the anisotropy field. In the samples studied here the coefficient of anisotropy is not high (about 5×10^4 J m^{-3}). M is the saturation magnetization. The frequency of the microwave field in these terms is $\Omega = \omega/\gamma H_i$.

Transmission of electromagnetic waves through a metallic ferromagnetic sample, the dispersion relations, and the conditions for the resonance of spin waves were studied in detail in [17, 18]. To analyse the change of the resonance with the introduction of hydrogen it is convenient to use the equations for the surface impedance obtained in these studies.

The anisotropic properties of the resonance frequency are regulated not only by the

orientation of $\boldsymbol{H}$ with respect to the sample plane but also by the equilibrium orientation of the magnetization in the sample with respect to $\boldsymbol{H}$. If the x- and z-axes are in the plane of the sample, $\boldsymbol{H}$ is rotated in the plane (x, y), and $\Theta_M = \Theta_H = \pi/2$ (ϕ_M, ϕ_H are the equilibrium orientations of $\boldsymbol{M}$ and $\boldsymbol{H}$ as determined by the condition of minimum free magnetic energy [16, 22, 23]):

$$2\eta \sin(\phi_M - \phi_H) = \sin 2\phi_M. \tag{4}$$

The anisotropy of the resonance frequency is determined, according to [22, 23], from the following equation:

$$\Omega^2 = [\eta \cos(\phi_H - \phi_M) + \cos 2\phi_M][\eta \cos(\phi_H - \phi_M) - \sin^2\phi_M]. \tag{5}$$

Although the anisotropy of the resonance fields is fully determined by relations (4) and (5), their values are provided via the solutions of the secular equation for the wave vector $\boldsymbol{K}$. These equations are presented in the appendix for the parallel and orthogonal orientations of the magnetic field with respect to the sample plane (formulas (A5) and (A6)). The equations (A1)–(A6) enable us to analyse the effect of material constants on the change of the resonance-field values. The analysis shows that for the case where $\varepsilon = 0$ the magnitude of the resonance field in the orthogonal orientation is equal to the frequency of the free Larmor precession Ω. In the case where $\varepsilon \neq 0$ and, at the same time, $\varepsilon \ll \eta$ and $L = 0$, the resonance field $\eta_\perp > \Omega$. For all of the cases $\eta_\parallel < \Omega$. $L \neq 0$ only causes the resonance field $\eta_\perp$ to become $< \Omega$, and

$$\frac{\Omega^2}{1 + L^2} = \eta_\parallel(\eta_\parallel + 1) \qquad \frac{\Omega}{1 + L^2} = \eta_\perp - 1. \tag{6}$$

Table 3. Values of the inherent magnetic induction $H_i = 4\pi M - H_A$ (the error is ± 0.005 T) obtained by means equations (5)–(7) and data from figure 3. Calculations are performed for the samples before hydrogen desorption ($t = 0$) and after prolonged hydrogen desorption ($t = t_1$, where the t_1 are given in table 1).

Number of the sample	$H_i(T)$	
	$t = 0$	$t = t_1$
N1	0.063	0.020
N2	0.216	0.020
N3	0.077	0.020
N4	0.060	0.023
N5	0.070	0.020
N6	0.023	0.023

Equations (4)–(6) and the experimental data in figure 3 for the resonance field enable us to obtain the values of the local induction H_i and the dimensionless damping constant L. The values of H_i are given in table 3.

Experiment shows that in the $Fe_{55}Cr_{25}Ni_{20}$ noncharged sample $H_\perp = 0.2022$ T is smaller than $\omega/\gamma = 0.3200$ T, but after introducing hydrogen into the sample the picture becomes the opposite: $H_\perp > \omega/\gamma$ (see table 1). Such behaviour of η under the influence of hydrogen attests to a significant decrease of the magnetization damping constant. In fact, using (6) we have found that $L = 1.04$ for the noncharged sample and $L = 0.2 \pm 0.05$ for the hydrogen-charged one. Therefore, the hydrogen atoms make magnetization of the sample more homogeneous. Apart from this, the value of the saturation magnetization is increased in the presence of hydrogen, which is revealed by the change of the shift in value

of the resonance fields $H_{\parallel}$, $H_{\perp}$ and the intensity of the FMR signal being proportional with the change of hydrogen concentration in the sample during desorption. From table 3 one can see the change of the local induction values in the sample, $H_i = 4\pi M - H_A$.

The anisotropy of the width of the FMR signal shown in figure 3 has a shape typical for thin metallic samples with weak inhomogeneous ferromagnetism. The signal width is mainly determined by three contributions: the exchange scattering of electrons by hydrogen atoms, independent of orientation but proportional to hydrogen concentration; the distribution of orientations of magnetization in the sample; and the inhomogeneity of local magnetic induction values.

Let us expand the signal width ΔH_{p-p} in terms of the small deviations $\langle \delta\phi \rangle$ and $\langle \delta H_i \rangle$ where ϕ is the angle between the magnetic moment and the external magnetic field:

$$\Delta H_{p-p} = \langle \delta H_0 \rangle + \langle \delta\phi \rangle \frac{\partial H_{\mathrm{res}}}{\partial \phi} + \langle \delta H_i \rangle \frac{\partial H_{\mathrm{res}}}{\partial H_i}. \tag{7}$$

Equations (4) and (5) for the resonance field allow one to find $\partial H_{\mathrm{res}}/\partial\phi$ and $\partial H_{\mathrm{res}}/\partial H_i$, and to evaluate the mean values of the three contributions in (7). The following data were obtained for sample N3:

$$\langle \delta H_0 \rangle = 0.1285 \text{ T} \qquad \langle \delta H_i \rangle = 0.02 \text{ T} \qquad \langle \delta\phi \rangle = 0.32^{\circ}. \tag{8}$$

Thus, the isotropic scattering of electrons provides the main contribution to the FMR signal width in the hydrogen-charged sample. As ΔH_{p-p} becomes markedly smaller than $\langle \delta H_0 \rangle$ during hydrogen desorption (see table 1, sample N3), hydrogen atoms must be the scattering centres for electrons.

Three main facts indicate the growing role of s electrons in the formation of the magnetic structure in hydrogenated austenite: (i) the resonance field is close to the value of ω/γ; (ii) the magnetization becomes stronger; and (iii) the magnetization becomes more homogeneous. At the same time the $T^{3/2}$-law for magnetization $M(T)$ is determined by the d-electron subsystem. This allows us to reach some conclusions about the type of hydrogen-induced magnetism. A strong s–d interaction between the spin-unpaired s electron of the hydrogen atom and d electrons of the host atoms leads to the creation of extended areas of enhanced spin polarization in the vicinity of the hydrogen atom. Spin–spin correlation binds these areas over the whole crystal if the average distance between hydrogen atoms is sufficiently small (see also section 4.2).

The temperature dependence of the signal integral intensity in figure 4 shows that the hydrogen desorption process doubles the contribution of hydrogen concentration to the $I(t)$ function. On the one hand, the saturation magnetization at $T = 0$ is changed; on the other, the Curie temperature decreases with the decrease of hydrogen concentration. One has to expect, as a result, that the $I(t)$ will turn out to be multiexponential functions. In fact, a double exponent is obtained for short time periods. Taking this into account, for higher reliability we measured $\Delta H_{p-p}(t)$ which is proportional to the hydrogen concentration. As follows from figure 6, the two functions, $\omega_I(t)$ and $\omega_{\delta H}(t)$, provide the same activation enthalpy for the jumps of the hydrogen atoms.

4.2. The enthalpy of activation and the frequency factor

The fact that the activation enthalpy obtained from the temperature–time measurements is consistent with the enthalpy of hydrogen migration in austenite gives strong evidence that the rate of hydrogen desorption from the samples is controlled by migration of the hydrogen atoms in the FCC crystal lattice. The value of the pre-exponential (frequency) factor in this

case characterizes the diffusion length of a hydrogen atom which leads to a detectable change of magnetic structure.

Three scale factors essentially affect the change of the FMR signal: (1) the length of the microwave-field inhomogeneity in the sample characterized by the depth of the skin layer in the alloy studied; (2) the inhomogeneity of the hydrogen atom distribution; and (3) the length of the magnetic inhomogeneity determined by the length of the electron spin–spin correlation.

In accordance with the diffusion theory, the ratio of the frequency factor obtained in [12–15] to the one in this study allows one to find the diffusion length of hydrogen atoms, l_d, which is crucial for the change of magnetization in the sample in our experiments:

$$l_d = a_0(\omega_{00}/\omega_0)^{1/2} = 6 \times 10^{-5} \text{ cm} \tag{9}$$

where a_0 is the crystal lattice parameter. Thus, the value of the diffusion length l_d is within the following limits: $R_H \ll l_d \ll \delta$, where $R_H = 10^{-7}$ is the average distance between hydrogen atoms at their initial concentration†; $\delta = 3 \times 10^{-4}$ cm is the skin layer depth in this alloy [24]. Therefore, l_d does not characterize inhomogeneity of the microwave field or the distribution of hydrogen atoms in the crystal lattice. The value l_d characterizes the scale of the spin correlation length of s electrons responsible for the FMR signal. In other words, the small value of the frequency factor measured in the FMR studies reflects the distance of hydrogen atom migration which causes a detectable change in the hydrogen-induced magnetic structure. The FMR signal caused by hydrogen disappears when the hydrogen concentration achieves a crucial value with $R_H = 10^{-5}$. In contrast, in the IF studies of anelastic relaxation the frequency factor characterizes the migration distance of hydrogen for the given relaxation time. As shown in [15], the value of the IF frequency factor in hydrogenated austenite corresponds to one or several jumps of the hydrogen atom needed for the reorientation of different multi-atom complexes (noncubic defects in the FCC lattice).

We feel that it is important that the value of the activation enthalpy determined here is consistent with the data from other experiments [12–15] and that, at the same time, the value of the frequency factor is surprisingly small. The latter attests to the fact that the s electrons of hydrogen atoms are bound with the spin and electron densities of the host atoms and take part in the formation of the alloy magnetic structure provided that the distance between the hydrogen atoms is smaller than the length of the spin–electron correlation.

5. Conclusions

1. Hydrogen causes a new line in the FMR spectrum of $Fe_{55}Cr_{25}Ni_{20}$ alloy, which disappears in the course of hydrogen desorption.

2. Hydrogen dissolution in $Fe_{55}Cr_{25}Ni_{20}$ alloy increases the saturation magnetization and the Curie temperature. It is shown that the main contribution to the broadening of the hydrogen-induced FMR line is given by scattering of electrons by hydrogen atoms.

3. Hydrogen desorption results in the decrease of the integral intensity of the FMR signal and its narrowing. From measurements of the rates of decay of the FMR signal and change of its width the values of the activation enthalpy of desorption, 0.56 ± 0.02 eV, and the frequency factor, $\omega_0 = (3.0 \pm 0.1) \times 10^6$ s^{-1} were obtained. The activation enthalpy of hydrogen desorption is consistent with that for hydrogen migration in CrNi austenitic steels measured with the help of other experimental techniques, while the value of the frequency

† In fact, R_H is smaller on account of the higher concentration of hydrogen in the surface layer according to the hydrogen concentration profile introduced by cathodic charging (see, e.g., [10]).

factor is about seven orders of magnitude smaller than the one obtained from the internal-frequency measurements. The low value of the frequency factor and the fact of the effect of the hydrogen on the FMR signal itself prove that hydrogen atoms induce the areas of high spin polarization in their surroundings, and the linear size of these areas is about of the length of spin–spin correlation, $l_d \approx 10^{-5}$ cm.

Acknowledgments

This study was performed with the financial support of the State Committee on Science and Technology of the Ukraine, project No 4.3.11, and of the International Science Foundation, project No UA4000. The authors also thank Professor J Foct, Lille University I, France, for helpful discussion.

Appendix

The absorption of the microwave power is equal to

$$P = (c/4\pi)^2 h_{10} \operatorname{Re} Z \tag{A1}$$

where the complex impedance Z can be expressed through solutions of Maxwell equations and the Landau–Lifshitz equation in the following way:

$$Z = \sum_i K_i h_{1i}. \tag{A2}$$

h_{10} is the amplitude of the microwave field applied to the sample. h_{1i} are electromagnetic fields at the sample surface:

$$h_{1i} = (T_{i+1}R_{i+2} - T_{i+2}R_{i+1}) \Big/ \sum_i (T_{i+1}R_{i+2} - T_{i+2}R_{i+1}). \tag{A3}$$

The summation in (A3) is performed for a number of solutions of the secular equation for the wave vector K_i, $i = 1, 2, 3$. R and T in (A3) are expressed through the wave vectors K_i:

$$\begin{aligned} &R_i = K_i(K_i^2 - K_0^2) \qquad K_0^2 = 2\mathrm{i}\varepsilon^2 \qquad \varepsilon^2 = A/2\pi H_i^2 \delta^2 \\ &T_i = \frac{K_i[(K_i^2 - \eta)(K_i^2 - K_0^2) + K_0^2]}{\mathrm{i}\Omega + L(1 + \eta - K_i^2)}. \end{aligned} \tag{A4}$$

A is the constant of the exchange interaction.

The equation for the wave vector K has the following form for (a) the case when $\boldsymbol{H}$ parallel to the sample plane:

$$\begin{aligned} &(K^2 - K_0^2)(K^6 - C_1K^4 + C_2K^2 - C_3) = 0 \\ &C_1 = K_0^2 + 2\eta + 1 + 2L\Omega/(1 + L^2) \\ &C_2 = (\eta + 2K_0^2)(\eta + 1) - [\Omega/(1 + L^2)][\Omega + L(4\varepsilon^2 - \mathrm{i}(2\eta + 1))] \\ &C_3 = K_0^2[(\eta + 1)^2 - (\Omega/(1 + L^2))(\Omega - 2\mathrm{i}L(\eta + 1))] \end{aligned} \tag{A5}$$

and the following form for (b) the case of $\boldsymbol{H}$ orthogonal to the sample plane:

$$K^4 + K^2[\Omega/(\mathrm{i}L \pm 1) - \eta - K_0^2] - K_0^2[\Omega/(\mathrm{i}L \pm 1) - \eta - 1] = 0. \tag{A6}$$

References

[1] Bernstein I M and Thompson A W (ed) 1973 *Hydrogen in Metals 1973; Proc. Int. Conf., TMS-AIME*
[2] Thompson A W and Moody N R (ed) 1990 *Hydrogen Effects on Material Behaviour 1990; Proc. 4th Int. Conf., TMS-AIME (Jackson Lake Lodge, WY)*
[3] Thompson A W and Moody N R (ed) 1994 *Proc. 5th Int. Conf., TMS-AIME (Jackson Lake Lodge, WY)*
[4] Quick N R and Johnson H H 1979 *Metall. Trans.* A **10** 67
[5] Brass A M, Chanfreau A and Chene J 1990 *Hydrogen Effects on Material Behaviour 1990; Proc. 4th Int. Conf., TMS-AIME (Jackson Lake Lodge, WY)* ed A W Thompson and N R Moody, p 19
[6] Inoue A, Hosoya Y and Matsumoto T 1979 *Trans. ISIJ* **19** 171
[7] Narita N, Altstetter C J and Birnbaum H K 1982 *Metall. Trans.* A **13** 1355
[8] Mathias H, Katz Y and Nadiv S 1978 *Met. Sci.* **12** 129
[9] Baranowski B, Majchrzak S and Flanagan T B 1971 *J. Phys. F: Met. Phys.* **1** 258
[10] Farrell K and Lewis M B 1981 *Scr. Metall.* **15** 661
[11] Ponyatowski E G, Antonov V E and Belash I T 1982 *Prog. Phys. Sci. (Usp. Phys. Nauk)* **137** 663 (in Russian)
[12] Asano S, Shibata M and Tsunoda R 1980 *Scr. Metall.* **14** 377
[13] Zielinski A 1990 *Acta Metall. Mater.* **38** 2573
[14] Gavriljuk V G, Hänninen H, Tarasenko A V and Ullakko K 1993 *Scr. Metall. Mater.* **29** 177
[15] Gavriljuk V G, Hänninen H, Tarasenko A V, Tereshchenko A S and Ullakko K 1995 *Acta Metall. Mater.* **43** 559
[16] Vonsovskij S V 1971 *Magnetism* ed 'Nauka' (Moscow: Nauka) p 1032 (in Russian)
[17] Patton C E 1976 *Czech J. Phys.* B **26** 925
[18] Fraitova D 1983 *Phys. Status Solidi* b **120** 341
[19] Shanina B D, Konchitz A A, Kolesnik S P, Gavriljuk V G and Tarasenko A V 1994 *Solid State Commun.* **90** 109
[20] Vonsovskij S V and Izjumov Yu A 1962 *Prog. Phys. Sci. (Usp. Phys. Nauk)* **77** 377 (in Russian)
[21] Sohmura T and Fujita F E 1980 *J. Phys. F: Met. Phys.* **10** 743
[22] Tjablikov S V 1965 *Methods of Quantum Theory of Magnetism* ed 'Nauka' (Moscow: Nauka) p 334 (in Russian)
[23] Smith J and Beljers H C 1955 *Philips Res. Rep.* **10** 113
[24] Gavriljuk V G, Efimenko S P, Smouk Ye E, Smouk S Yu, Shanina B D, Baran N P and Maksimenko V M 1993 *Phys. Rev.* B **48** 3224